Adsorption (2013) 19:455–463
DOI 10.1007/s10450-012-9467-2

Coordination of extraframework Li^+ cation in the MCM-22 and MCM-36 zeolite: FTIR study of CO adsorbed

Roman Bulánek · Monika Kolářová · Pavla Chlubná · Jiří Čejka

Received: 30 October 2012 / Accepted: 26 December 2012 / Published online: 16 January 2013

Abstract Nature and population of Li^+ cationic sites in MCM-22 zeolite and its pillared form (MCM-36) were investigated by means of adsorption of CO as a probe molecule. CO stretching frequency and adsorption heat were measured by FTIR spectroscopy and adsorption microcalorimetry. Intrazeolitic carbonyl complexes on Li^+ cations in MCM-22 and MCM-36 are characterized by two main vibrational bands at 2,195 and 2,188 cm^{-1}. Band at higher wavenumbers is ascribed to carbonyls on Li^+ ions coordinated only to two oxygen atoms at the intersection of 10-ring channels and interacting with CO molecule by energy around 45 kJ mol^{-1}. Band at 2,188 cm^{-1} was assigned to the carbonyls on Li^+ cations located on top of 5 or 6-rings on the channel walls and coordinated to three or four oxygen atoms, interacting with CO molecule by energy 33–36 kJ mol^{-1}. Effect of pillaring and layered form of zeolite on nature and population of Li^+ cationic sites is also discussed, as well as the formation of dicarbonyl complexes.

Keywords FTIR · CO · Adsorption microcalorimetry · MCM-22 · MCM-36

Abbreviations

FCC	Fluid catalytic cracking
C_{16}TMA-OH	Cetyltrimethylammonium hydroxide
HMI	Hexamethyleneimine
BET method	Brunauer–Emmett–Teller method
BJH method	Barrett–Joyner–Halenda method
FTIR	Fourier transform infrared spectroscopy
MCT/A	Mercury cadmium telluride IR detector
S_{BET}	BET Surface area (m^2 g^{-1})
V_{micro}	Micropore volume (cm^3 g^{-1})
V_{tot}	Total pore volume (cm^3 g^{-1})
ν_{CO}	Stretching frequency of C–O vibration (cm^{-1})
Q_{diff}	Differential adsorption heat (kJ mol^{-1})

R. Bulánek (✉) · M. Kolářová
Department of Physical Chemistry, Faculty of Chemical Technology, University of Pardubice, Studentská 573, 532 10 Pardubice, Czech Republic
e-mail: roman.bulanek@upce.cz

P. Chlubná · J. Čejka
J. Heyrovsky Institute of Physical Chemistry, Academy of Sciences of the Czech Republic, v.v.i., Dolejškova 3, 182 23 Prague, Czech Republic

1 Introduction

Knowledge of the localization and coordination of extraframework cations in zeolites is important for understanding their sorption properties (gas separation, gas storage) and potential catalytic activity. The structure and coordination of extraframework cations in aluminum-rich zeolites can be determined by X-ray and neutron diffraction analysis (Mortier 1982; Olson 1995). However, due to a low content of extraframework metal cations in high-silica zeolites and a relatively large number of accessible extraframework cation sites, the knowledge is lacking for these systems and, thus, information about the metal coordination can be obtained mainly from indirect experimental techniques, including spectroscopic characterization using probe molecules (Zecchina and Arean 1996). Infrared spectroscopy of adsorbed carbon monoxide is one of the most popular techniques for the investigation of extraframework charge balancing cations in zeolites (Zecchina and Arean 1996; Hadjiivanov and Vayssilov

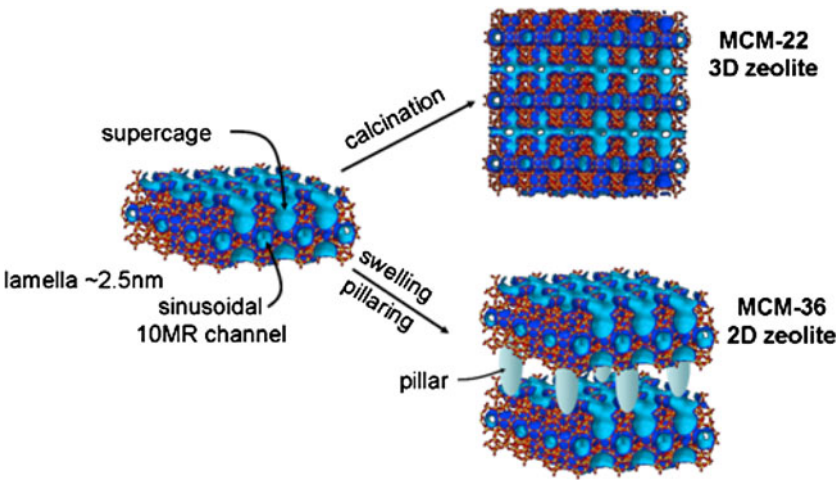

Fig. 1 Scheme of the MWW zeolite framework structure. Framework T atoms (Al or Si) and O atoms are depicted as *yellow* and *red* sticks, respectively. Surface of the zeolite channels and cavities is depicted by *blue* surface (*light* and *dark blue* is used for *inner* and *outer side* of channel surface) (Color figure online)

2002; Garrone and Arean 2005; Nachtigall et al. 2012). CO stretching frequencies and CO adsorption enthalpy are highly sensitive to the nature and environment of the adsorption site. Previously, (Nachtigallova et al. 2006) proposed a general model of CO vibrational dynamics in porous systems. It was reported that the small Li^+ cation is the most suitable cation for probing the site-specificity due to the effects from the bottom (primarily determined by the nature of the metal cation and its coordination to the zeolite framework) while the effect from the top (originating from interaction of oxygen atom of CO with charge on the opposite wall of zeolite channel or cavity, where negative charge of framework oxygen atoms or positive charge of second cation is located) is not site specific in the case of the Li^+ cations (Nachtigall et al. 2007; Nachtigall and Bulanek 2006). Increasing number of oxygen atoms, to which Li^+ cation is coordinated, led to weakening of the Li^+ interaction with CO and the lowering of the shift in ν_{CO}. Therefore, experimental determination of CO stretching frequency and adsorption enthalpy for particular zeolite can provide information on type of cationic adsorption sites present in the investigated zeolite.

MCM-22 zeolite (IZA code-MWW) possesses the unique layered structure with two independent 10-ring pore systems, the intralayer sinusoidal channel (with dimensions of 4.0 × 5.5 Å) and the interlayer pore comprised of large supercage (inner diameter 7.1 Å and height of 18.2 Å) defined by 12-rings and connected by 10-ring with dimensions 4.1 × 5.1 Å (see Fig. 1) (Leonowicz et al. 1994; Dorset et al. 2005). Synthesis of MCM-22 proceeds via a layered precursor (Lawton et al. 1996). The complete three-dimensional structure is formed by condensation of the individual layers. The discovery of a layered form of the catalytically active zeolite MCM-22 was exploited for synthesis of pillared zeolite (MCM-36) combining unprecedented mesoporous structure and high zeolite activity (Roth et al. 1995). Presence and accessibility of cationic sites in supercages on the external surface of MCM-22 has been postulated to play a significant role in catalytic processes (Lawton et al. 1998).

This zeolite family attracts a particular attention owing to its adsorption and catalytic properties. MWW zeolite has been proved to be catalytically active in alkylation of benzene and cracking of n-alkanes, it is also used as an FCC octane booster additive especially valuable for the production of reformulated gasolines (Corma et al. 1997, 2000, 1999; Cejka et al. 2002; Roth and Cejka 2011). MCM-22 zeolite containing Cu^+ cations exhibited also remarkable activity and stability in the decomposition of NO and N_2O in the presence of water, whereas CuZSM-5 deactivated rapidly upon steaming (Palella et al. 2004). Adsorption of different adsorptive as carbon dioxide, nitrosamines or basic dyes was also investigated (Zukal et al. 2009a, b; Pawlesa et al. 2007; Corma et al. 1996; Yang et al. 2010, 2012; Wang et al. 2006; Grajciar et al. 2012). Despite the previously mentioned unique catalytic and adsorption properties of these zeolites, studies of cation coordination and localization in MWW framework are rather rare. The largest attention has been paid to the characterization of acidic sites and monovalent copper cations in MCM-22 zeolite (Onida et al. 1999; Umamaheswari et al. 2005; Milanesio et al. 2008).

In this contribution, we investigate coordination of Li^+ cation in MCM-22 and MCM-36 zeolite framework by the study of CO adsorption on these materials. The purpose of this study is twofold. On the one hand, it is of an interest to gather detail knowledge about very promising catalytic system and adsorbent. On the other hand, the comparison of MCM-22 and MCM-36 may help to understand the structure of the external surface of a zeolite which is playing important role in many catalytic reactions.

2 Experimental

MCM-22 precursor (MCM-22P) was synthesized by following procedure: 1.16 g of NaOH was dissolved in 251.2 g of water and mixed with 1.68 g of sodium aluminate (40–45 % Na_2O, 50–56 % Al_2O_3). Then, 62 g of LUDOX (AS 30) was added. The mixture became thick and was stirred until homogeneous gel was formed. Then, 17.2 g of hexamethylenimine (HMI) was added and the final mixture was stirred for 2 h. The reaction mixture was charged into Teflon-lined steel autoclaves (4 × 90 ml). Crystallization proceeded at 150 °C under agitation and autogeneous pressure for 5 days. Solid product was collected by filtration, washed with distilled water and dried in the oven at 60 °C overnight.

Part of MCM-22P was calcined at 540 °C for 6 h with temperature ramp of 2 °C min^{-1}. The calcined product MCM-22 was ion-exchanged into NH_4^+ form by treating four-times with 1.0 M NH_4NO_3 solution for 4 h at room temperature (100 ml of solution/1 g of zeolite).

Second part of MCM-22P (3.8 g of uncalcined MCM-22P sample) was mixed with 77 ml of ion-exchanged cetyltrimethylammonium hydroxide (C_{16}TMA-OH) and the slurry was stirred overnight at ambient temperature. The product was separated by centrifugation, properly washed out with distilled water and dried at 60 °C. Pillaring was carried out with 5 g of swollen MCM-22 in 150 ml of tetraethyl orthosilicate (1 g of zeolite per 30 ml of TEOS). The mixture was stirred and heated under reflux at 85 °C for overnight. The solid was isolated by centrifugation, dried at 40 °C and hydrolyzed by adding about 500 ml of water to 5.013 g of dried powder (stirred overnight at room temperature). The product was centrifuged again and dried at 60 °C. Final calcination was carried out at 540 °C for 6 h with the temperature ramp of 2 °C min^{-1}. The calcined product MCM-36 was ion-exchanged into NH_4^+ form by treating four-times with 1.0 M NH_4NO_3 solution for 4 h at room temperature (100 ml of solution/1 g of zeolite). Li^+ form of zeolites was prepared by conventional ion-exchange from aqueous solution of 1 M LiCl at 45 °C for 5 days.

Concentration of exchangeable cations was determined by quantitative analysis of ammonia evolved from NH_4^+ form of zeolites during ammonia temperature programmed desorption. Chemical analysis of the samples is summarized in the Table 1.

All as-synthesized, calcined and ion-exchanged samples were checked for their crystallinity and phase purity by X-ray powder diffraction on a Bruker D8 X-ray powder diffractometer equipped with a graphite monochromator and position sensitive detector (Våntec-1) using CuKα radiation (at 40 kV and 30 mA) in Bragg–Brentano geometry. The size and shape of synthesized materials were evaluated by scanning electron microscopy images using a JEOL JSM-5500LV instrument.

Nitrogen adsorption/desorption isotherms at −196 °C on zeolites under study were recorded using GEMINI II 2370 instrument (Micromeritics). Before the sorption measurements all samples were degassed under helium at 200 °C for 4 h. The specific surface area was evaluated by BET method and the mesopore size distribution was calculated using BJH method.

Prior to IR spectra measurement, the samples were pressed into self-supporting wafers with surface density of about 10 mg cm^{-2} and placed into IR cell for transmission measurement. The zeolite samples were in situ activated (outgassed) in a dynamic vacuum (residual pressure $<10^{-4}$ Torr) for 10 h at 430 °C (with rate of temperature increase 5 °C min^{-1} from ambient to required temperature). Infrared spectra (64 scans) of carbonylic species formed upon adsorption of CO were collected with a resolution of 2 cm^{-1} on a Nicolet 6700 FTIR spectrometer equipped with an MCT/A cryodetector. CO was adsorbed on the samples at liquid nitrogen temperature under equilibrium pressure of 0.5 Torr. Subsequently, IR spectra were collected while the surface coverage was decreasing due to evacuation at the same temperature. IR spectrum of empty IR cell was taken as a background for each measured spectrum. The spectrum of dehydrated sample recorded before CO adsorption was subtracted from each spectrum shown in this work. All spectra were normalized to wafer surface density of 10 mg cm^{-2} using integral intensity of zeolite skeletal overtones (2,066–1,721 cm^{-1}) as a benchmark. The Si/Al ratio was determined using adsorption of pyridine (PYR) followed by IR spectroscopy (Nicolet Protégé with a transmission DTGS and MTC/A detector). Before adsorption, pyridine was degassed by freeze-and-thaw cycles. Pyridine was adsorbed at 150 °C for 20 min at partial pressure 600–800 Pa, followed by desorption for 20 min. All spectra were recorded with a resolution of 2 cm^{-1} by collecting 128 scans for a single spectrum at room temperature. Spectra were recalculated to a wafer density of 10 mg cm^{-2}.

Table 1 Chemical analysis and textural characteristics of the MWW zeolites

Zeolite	Si/Al	n_{Li} (mmol g^{-1})	S_{BET} (m^2 g^{-1})	V_{micro} (cm^3 g^{-1})	V_{tot} (cm^3 g^{-1})
MCM-22	24.5	0.395	447	0.17	0.26
MCM-36	29.9	0.293	637	0.11	0.32

Calorimetric measurements were carried out using isothermal microcalorimeter of Tian-Calvet type (BT 2.15, Setaram) operating at −100 °C connected with home-made volumetric–manometric device. Prior to each measurement, the samples of the weight of 400 mg were outgassed by the same procedure as in the case of IR spectra measurements. Experimental set-up represents open isothermal system. The free volume of the apparatus was determined by set of expansion experiments with helium as an inert/nonadsorbing gas at different pressure ranges. The adsorption isotherms were measured via step-by-step introduction of adsorptive into the cell. The CO (purity of 99.997 % supplied by Linde Gas Corp.) was introduced via a system of electrically operated vacuum valves controlled by PC with software developed at our laboratory. Once pressure in the dosing volume was stabilized, the valve separating dosing volume from sample cell was opened to allow the adsorptive to reach the sample. The system was equilibrated at each dose for 50 min. All experiments consist of minimally 40 dosing cycles. More details about calorimetric measurements are published in our previous papers (Bulanek et al. 2010, 2011).

3 Results and discussion

X-ray powder diffraction patterns of the parent MCM-22 (black patter) and MCM-36 (red pattern) samples (Fig. 2) confirmed good crystallinity of the matrices. Compared with the pattern of MCM-22, an intense low-angle peak appears at 1.95° 2θ in the XRD pattern of MCM-36 corresponding to a d-spacing of 4.53 nm, which represents the new c-parameter of the unit cell. This d-value includes the c-parameter of the unit cell of MCM-22 and the spacing distance between the layers of MCM-36. The distance between two layers in MCM-36 is calculated by subtracting the thickness of the layer (c-parameter of MCM-22, 2.51 nm; Leonowicz et al. 1994). The values obtained for the samples suggest an average interlayer distance of 2.02 nm. All peaks observed correspond perfectly to those of the MCM-36 material reported by Roth et al. (1995). SEM micrographs (Fig. 3) of the parent matrices show typical sheets like discs or agglomerates of a number of cross-linked discs (Corma et al. 1995; Nicolopoulos et al. 1994). The N_2 adsorption/desorption isotherms of MCM-22 and MCM-36 parent materials are shown in Fig. 4. The surface areas (S_{BET}), micropores volume (V_{micro}) and total pore volume (V_{tot}) are summarized in the Table 1. Surface area of pillared zeolite is significantly larger than surface area of MCM-22 as well as total pore volume. This is in agreement with data reported in literature and with the fact that additional surface of pillared lamellas exists in the MCM-36 sample (Laforge et al. 2005; Meloni et al. 2001; Pawlesa et al. 2007). Both isotherms exhibit an H4 hysteresis loop according to IUPAC classification. This type of hysteresis loop is usually related to slit-shape pores among plate-like particles. This is in accordance with morphology of studied samples (see Fig. 3). The micropore volumes were determined using t-plot method. The value of V_{micro} of pillared zeolite is significantly lower than V_{micro} of MCM-22 zeolite. The IR spectra of OH groups of the H– and Li– form of both zeolites exhibit three distinguished signals (Fig. 5) in agreement with previous studies (Onida et al. 1999; Corma et al. 1995). The sharp band centered at 3,750 cm^{-1} is assigned to isolated silanols mainly located on the external surface of the zeolite crystals. The weak absorption band at 3,675 cm^{-1} is ascribed to the AlOH species partially anchored to the zeolitic framework. The absence of broad absorption band at about 3,500 cm^{-1} suggests a negligible presence of hydroxyl nests and thus structure imperfections. The band at 3,626 cm^{-1} corresponds to the bridged hydroxyl groups (Si(OH)Al), therefore to the Broensted acid sites and exchangeable protons in the zeolite. The band corresponding to Broensted acid sites is completely missing in the spectra of Li– form of both zeolites evidencing the complete ion-exchange of H–form to provide the lithium form.

Figure 6 shows IR spectra recorded at liquid nitrogen temperature concerning the adsorption of CO on Li-MCM-22 (Fig. 6a) and Li-MCM-36 (Fig. 6b). To compare FTIR and calorimetric data, the experimental results are discussed first for the lowest surface coverage (reflecting the most stable adsorption species) followed by spectra obtained for increasing coverages. At low CO coverages, the spectra of CO/Li-MCM-22 (Fig. 6a) are dominated by the band at 2,195 cm^{-1}. This band represents the most stable carbonyl complexes. However, it is apparent that

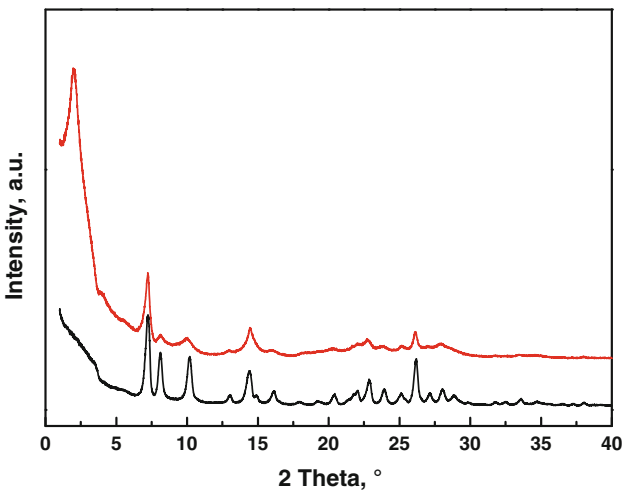

Fig. 2 X-ray diffraction patterns of the calcined NH_4^+ forms of MCM-22 (*black curve*) and MCM-36 (*red curve*) parent zeolites (Color figure online)

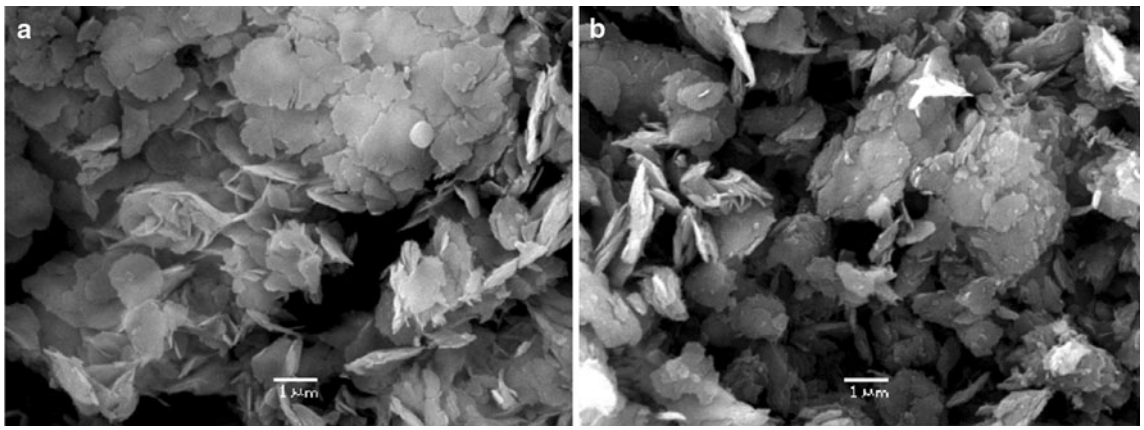

Fig. 3 Scanning electron micrographs of parent calcined NH_4^+-MCM-22 (**a**) and NH_4^+-MCM-36 (**b**) zeolite

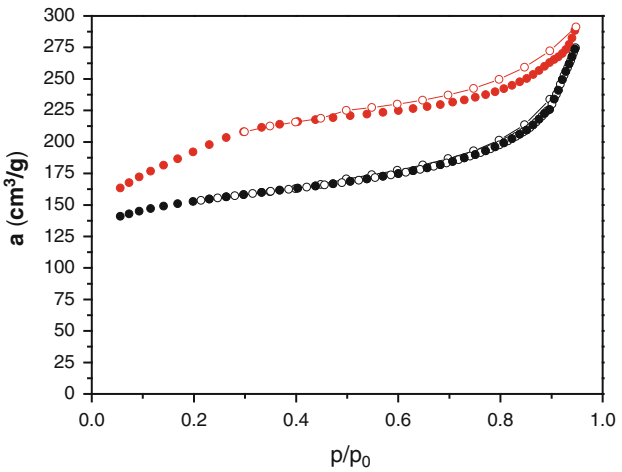

Fig. 4 Nitrogen adsorption isotherms of parent calcined MCM-22 (*black points*) and MCM-36 (*red points*) zeolite (*open symbols* for desorption, *full symbol* for adsorption) (Color figure online)

even at very low CO coverage the spectra are not symmetrical showing a weak band at about 2,188 cm^{-1}. The respective sites become more populated. Detailed inspection of the spectra reveals that high-frequency band keeps a constant wavenumber, whereas the low-frequency band shifts with increasing coverage by about 3 cm^{-1} to lower frequency. Features of spectra reported here resemble spectra of Li–CO complexes in Li-ZSM-5 reported in the literature before (Bonelli et al. 2003; Nachtigallova et al. 2004; Nachtigall et al. 2007). The similarities of cation coordination in MCM-22 and ZSM-5 were also reported by Umamaheswari et al. 2005 based on similarities in spectroscopic characteristics of EPR signals of Cu(I)–NO complexes in Cu-MCM-22 and Cu-ZSM-5 zeolites. Previously, on the basis of a good agreement between experimental IR spectra and theoretical calculations obtained for a number of different Li exchanged zeolites, four types of stable Li^+ sites in zeolites were discussed and

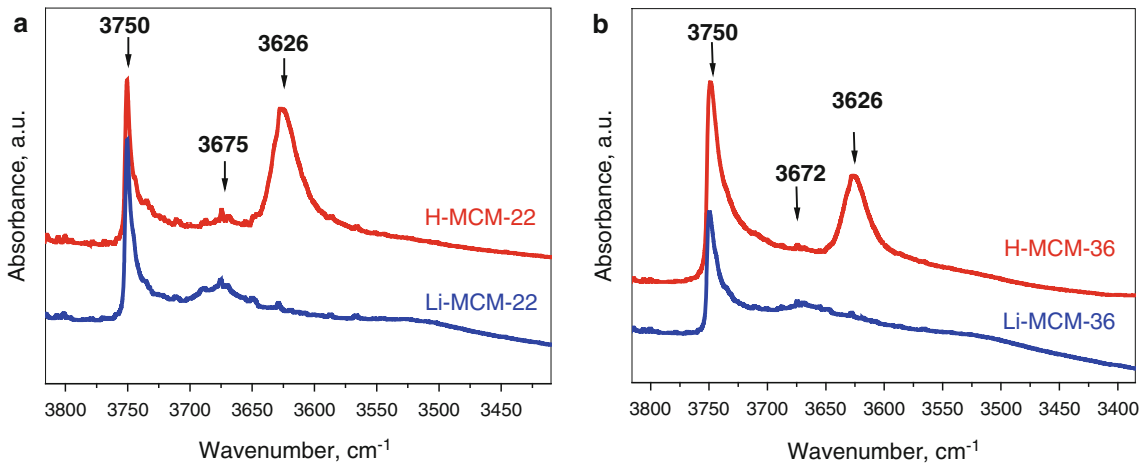

Fig. 5 FTIR spectra of OH stretching vibration region of dehydrated MCM-22 (**a**) and MCM-36 (**b**) zeolite. H-forms of samples resulting from calcination of parent zeolites are depicted by *red lines* and Li-forms are depicted by *blue lines* (Color figure online)

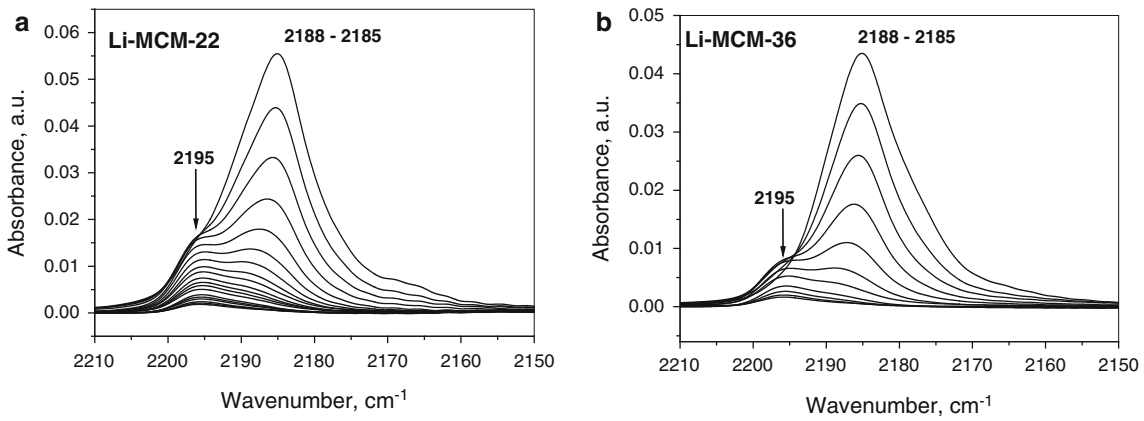

Fig. 6 FTIR spectra of CO adsorbed at liquid nitrogen temperature on the sample Li-MCM-22 (**a**) and Li-MCM-36 (**b**) under dynamic vacuum

characterized by stretching frequency of corresponding carbonyl complexes (Nachtigall et al. 2007): (i) Li^+ ions coordinated only to two oxygen atoms at the intersection of two 10-ring channels; corresponding to monocarbonyl complexes are characterized by $\nu_{CO} > 2{,}190$ cm^{-1}. (ii) Li^+ ions coordinated to three oxygen atoms of 8-ring or Li^+ cation located on top of 5 or 6-rings on the channel walls and coordinated to three or four oxygen atoms; corresponding monocarbonyl complexes are characterized by $\nu_{CO} \sim 2{,}187$ cm^{-1}. (iii) Li^+ cations located in the plane of 6-ring and coordinated to four oxygen atoms of this ring; corresponding monocarbonyl complexes are characterized by $\nu_{CO} \sim 2{,}182$ cm^{-1} and (iv) Li^+ cations in the vicinity of two framework aluminium atoms (Al-pair); corresponding monocarbonyl complexes are characterized by $\nu_{CO} \sim 2{,}170$ cm^{-1}. The experimental spectra of Li-MCM-22 (Fig. 6a) can be interpreted in the light of general characteristics of carbonyl complexes mentioned above: the 2,195 and 2,188 cm^{-1} bands are due to CO adsorption on the Li^+ cations coordinated only to two oxygen atoms and localized at intersection of sinusoidal 10-ring channel and supercage and the Li^+ cations coordinated to three or four oxygen atoms of the zeolite framework on the wall of zeolite channels, respectively. Presence of two Al atoms in close vicinity of Li^+ cation leads to decrease in partial charge of the Li^+ cation and subsequently to the lowering of interaction energy and stretching frequency of carbonyl complex formed on this Li^+ cation. Considering very low intensity of the spectra below 2,175 cm^{-1}, we can claim that investigated samples contain only very insignificant amount of Li^+ cations in the vicinity of two framework aluminium atoms (Al-pair). This observation is in agreement with high Si/Al ratio of investigated sample (Si/Al = 24.5) limiting a presence of Al-pair in the framework. Shift of the band at 2,188 cm^{-1} with increasing CO coverage to 2,185 cm^{-1} can be due to the formation of dicarbonyl complexes or due to the formation of Li^+ carbonyls on cations located in the plane of 6-ring and coordinated to four oxygen atoms, which exhibit lower stability of carbonyl complexes. The calculated CO stretching frequencies of dicarbonyl complexes in Li-ZSM-5 zeolite are 3–13 cm^{-1} lower than ν_{CO} of monocarbonyl complexes (Nachtigallova et al. 2004). Geminal species in the alkali-metal exchanged zeolites behave as two independent (or very weakly coupled) oscillators showing only one vibrational band in the IR spectrum, as documented in the literature (Hadjiivanov et al. 2001; Hadjiivanov and Knozinger 1999; Arean et al. 2001; Bonelli et al. 2003). Theoretical calculation of the splitting of CO frequencies in $Li^+(CO)_2$ complexes (1T model, C_{2v} symmetry) reported in the literature showed that the split of both vibrational modes was less than 2 cm^{-1} at all levels of theory (Nachtigallova et al. 2004). The theoretical study of Li-ZSM-5 (Sillar and Burk 2007) and Li-FER (Nachtigall and Bulanek 2006) zeolites led to the conclusion that dicarbonyls can be formed mainly on the Li cations at the channel intersections with the adsoption enthalpy for the second CO molecule being only about 50–75 % that of adsorption enthalpy of the first CO molecule, it means in the range from 34 to 23 kJ mol^{-1}. Ability of Li^+ cations in MCM-22 zeolite to form dicarbonyls is evidenced by CO adsorption isotherms and calorimetric measurements reported here later (see Fig. 7).

FTIR spectra of CO adsorbed on Li-MCM-36 are depicted in the Fig. 6b. Intensities of CO vibrational bands in the spectra are approximately about 80 % that of MCM-22 in accordance with Si/Al ratio and Li^+ concentration in individual samples. It is evident by comparison of IR spectra in Fig. 6b that the main spectral features are identical with IR spectra of intrazeolitic carbonyls formed on Li-MCM-22 zeolite (Fig. 6a). The changes of positions and intensities of the bands with CO coverage are the same as in the case of Li-MCM-22. Therefore, this observation indicates that swelling of layered precursor of MCM-22P

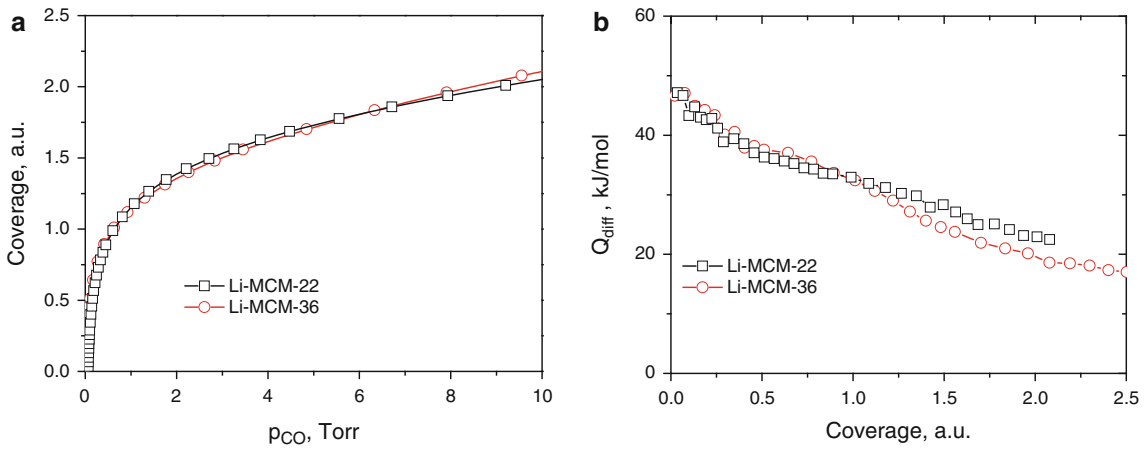

Fig. 7 CO adsorption isotherms (**a**) and differential heats of CO adsorption as a function of adsorbed amount (**b**) concerning the CO adsorption at −100 °C on the sample Li-MCM-22 (*black points*) and Li-MCM-36 (*red points*) (Color figure online)

and its subsequent pillaring did not affect the coordination and localization of Li^+ cations. Split of supercage and existence of mesoporous space between individual lamellas did not lead to formation of new Li sites, disappearance of some specific Li sites or alteration of effect from the top (interaction of CO with opposite channel wall). This means that Li cationic sites in the MWW zeolite framework are located in the sinusoidal 10-ring channel or are deeply sunk in the cups of supercage.

Figure 7 reports both the volumetric isotherms and calorimetric curve (differential heats of adsorption vs. coverage) for both investigated Li-zeolites. The curves corresponding to Li-MCM-22 and Li-MCM-36 sample in both plots closely overlap. This agrees with similarities of IR spectra and confirms conclusion drawn from comparison of stretching frequencies of carbonyls on both samples. Adsorption isotherms exhibit steep concave shape. The monolayer capacity was achieved at CO equilibrium pressure 0.6 Torr. Subsequent increase in CO pressure led to gradual increase in the adsorbed amount proving the formation of dicarbonyl complexes under these conditions (−100 °C and CO pressure above 0.6 Torr). The initial differential heat of adsorption is 47 kJ mol^{-1}, which coincides with the value of 45 kJ mol^{-1} predicted by theoretical calculation (interaction energy of −32 kJ mol^{-1} obtained from DFT calculation at 0 K for two coordinated Li cations (Nachtigall et al. 2007) plus contribution of dispersive interaction being estimated to be around 13 kJ mol^{-1}). Comparison of calorimetric and FTIR results led to the conclusion that this adsorption heat characterizes carbonyls reflected in vibrational band at 2,195 cm^{-1} because this band prevails in the spectra at very low coverage. The differential heat of adsorption is seen to decrease gradually with coverage to value of 33 kJ mol^{-1} at monolayer. This is consistent with adsorption heats of CO interacting with Li^+ cation located on top of 5 or 6-rings on the channel walls and coordinated to three or four oxygen atoms, which was predicted to be 33–36 kJ mol^{-1} (taking into account contribution of dispersive interaction of 13 kJ mol^{-1}). This adsorption heat characterizes carbonyl species represented in the IR spectra by band at 2,188 cm^{-1} because this band is populated at coverage close to monolayer. Adsorption of CO on Li^+ cations above monolayer capacity is characterized by adsorption heat ranging from 33 to 23 kJ mol^{-1} being in a very good agreement with theoretical prediction that adsorption enthalpy for the second CO molecule is only about 50–75 % that of adsorption enthalpy of the first CO molecule. Dicarbonylic species are formed preferentially on the intersection sites characterized by adsorption heat around 47 kJ mol^{-1}, therefore the heat of 33 kJ mol^{-1} represents 70 % of this value. Last dicarbonylic species are formed on channel wall sites characterized by adsorption heat 33–36 kJ mol^{-1}. The value of 23 kJ mol^{-1} represents also 70 % of adsorption heat of monocarbonyls on these sites. It must be noted that adsorption isotherms did not level off at coverage equal to 2, therefore we cannot exclude formation of some tricarbonylic species but probability of such species formation is relatively low.

4 Conclusion

To the best of our knowledge, nature of cationic sites of conventional 3D MCM-22 zeolite and its pillared lamellar form (MCM-36) was characterized and compared for the first time. By combining FTIR spectroscopic and microcalorimetric measurements on adsorbed CO, at least two lithium sites were identified to be present in the Li-MCM-22 and Li-MCM-36 zeolites. Intrazeolitic carbonyls on Li^+ cations in MCM-22 and MCM-36 are characterized by two main vibrational bands at 2,195 and 2,188 cm^{-1}.

High-frequency band is ascribed to carbonyls on Li^+ ions coordinated only to two oxygen atoms at the intersection of two 10-ring channels. Band at 2,188 cm^{-1} is assigned to carbonyls on Li^+ cations located on the top of 5 or 6-membered rings on the channel walls and coordinated to three or four oxygen atoms, respectively. This is in line with the heat of adsorption of CO on investigated samples ranging from 47 kJ mol^{-1} at zero coverage to 33 kJ mol^{-1} at monolayer coverage. Slight shift of low-frequency band in IR spectra from 2,188 to 2,185 cm^{-1} is an indication of the formation of dicarbonylic complexes (in agreement with reaching coverage higher than monolayer). Comparison of FTIR spectra and calorimetric curves for both conventional 3D (MCM-22) and lamellar 2D (MCM-36) zeolite led to conclusion that swelling and pillaring of MCM-22 precursor does not cause the formation of new cationic sites nor leads to the disappearance of some specific cationic site. From this it can be deduced that Li cationic sites are localized on the 10-ring channel walls or at the bottom of the cups of zeolite supercage.

Acknowledgments The authors thank to the Czech Science Foundation for financial support of the project of Centre of Excellence no. P106/12/G015 InDeNAC (www.zeolites.cz).

References

Arean, C.O., Manoilova, O.V., Delgado, M.R., Tsyganenko, A.A., Garrone, E.: Formation of several types of coordination complexes upon CO adsorption on the zeolite Li-ZSM-5. Phys. Chem. Chem. Phys. **3**(19), 4187–4188 (2001)

Bonelli, B., Garrone, E., Fubini, B., Onida, B., Delgado, M.R., Arean, C.O.: Two distinguishable lithium sites in the zeolite Li-ZSM-5 as revealed by adsorption of CO: an infrared spectroscopic and thermodynamic characterisation. Phys. Chem. Chem. Phys. **5**(13), 2900–2905 (2003)

Bulanek, R., Frolich, K., Frydova, E., Cicmanec, P.: Microcalorimetric and FTIR study of the adsorption of carbon dioxide on alkali-metal exchanged FER zeolites. Top. Catal. **53**(19–20), 1349–1360 (2010). doi:10.1007/s11244-010-9593-6

Bulanek, R., Frolich, K., Frydova, E., Cicmanec, P.: Study of adsorption sites heterogeneity in zeolites by means of coupled microcalorimetry with volumetry. J. Therm. Anal. **105**(2), 443–449 (2011). doi:10.1007/s10973-010-1108-y

Cejka, J., Krejci, A., Zilkova, N., Kotrla, J., Ernst, S., Weber, A.: Activity and selectivity of zeolites MCM-22 and MCM-58 in the alkylation of toluene with propylene. Microporous Mesoporous Mater. **53**(1–3), 121–133 (2002)

Corma, A., Corell, C., Perezpariente, J.: Synthesis and characterization of the MCM-22 zeolite. Zeolites **15**(1), 2–8 (1995). doi:10.1016/0144-2449(94)00013-i

Corma, A., Corell, C., PerezPariente, J., Guil, J.M., GuilLopez, R., Nicolopoulos, S., Calbet, J.G., ValletRegi, M.: Adsorption and catalytic properties of MCM-22: the influence of zeolite structure. Zeolites **16**(1), 7–14 (1996). doi:10.1016/0144-2449(95)00084-4

Corma, A., Davis, M., Fornes, V., GonzalezAlfaro, V., Lobo, R., Orchilles, A.V.: Cracking behavior of zeolites with connected 12- and 10-member ring channels: the influence of pore structure on product distribution. J. Catal. **167**(2), 438–446 (1997). doi:10.1006/jcat.1997.1584

Corma, A., Diaz, U., Fornes, V., Guil, J.M., Martinez-Triguero, J., Creyghton, E.J.: Characterization and catalytic activity of MCM-22 and MCM-56 compared with ITQ-2. J. Catal. **191**(1), 218–224 (2000). doi:10.1006/jcat.1999.2774

Corma, A., Fornes, V., Martinez-Triguero, J., Pergher, S.B.: Delaminated zeolites: combining the benefits of zeolites and mesoporous materials for catalytic uses. J. Catal. **186**(1), 57–63 (1999). doi:10.1006/jcat.1999.2503

Dorset, D.L., Roth, W.J., Gilmore, C.J.: Electron crystallography of zeolites—the MWW family as a test of direct 3D structure determination. Acta Crystallogr. Sect. A **61**, 516–527 (2005). doi:10.1107/s0108767305024670

Garrone, E., Arean, C.O.: Variable temperature infrared spectroscopy: a convenient tool for studying the thermodynamics of weak solid–gas interactions. Chem. Soc. Rev. **34**(10), 846–857 (2005)

Grajciar, L., Cejka, J., Zukal, A., Arean, C.O., Palomino, G.T., Nachtigall, P.: Controlling the adsorption enthalpy of CO_2 in zeolites by framework topology and composition. Chemsuschem **5**(10), 2011–2022 (2012). doi:10.1002cssc.201200270

Hadjiivanov, K., Knozinger, H.: FTIR spectroscopic evidence of formation of geminal dinitrogen species during the low-temperature N-2 adsorption on NaY zeolites. Catal. Lett. **58**(1), 21–26 (1999)

Hadjiivanov, K., Knozinger, H., Ivanova, E., Dimitrov, L.: FTIR study of low-temperature CO and N-15(2) adsorption on a CaNaY zeolite: formation of site-specified Ca^{2+} (CO)(3) and Ca^{2+} (N-15(2))(3) complexes. Phys. Chem. Chem. Phys. **3**(12), 2531–2536 (2001)

Hadjiivanov, K.I., Vayssilov, G.N.: Characterization of oxide surfaces and zeolites by carbon monoxide as an IR probe molecule. Adv. Catal. **47**(47), 307–511 (2002)

Laforge, S., Ayrault, P., Manin, D., Guisnet, M.: Acidic and catalytic properties of MCM-22 and MCM-36 zeolites synthesized from the same precursors. Appl. Catal. A **279**(1–2), 79–88 (2005). doi:10.1016/j.apcata.2004.10.015

Lawton, S., Leonowicz, M.E., Partridge, R., Chu, P., Rubin, M.K.: Twelve-ring pockets on the external surface of MCM-22 crystals. Microporous Mesoporous Mater. **23**(1–2), 109–117 (1998). doi:10.1016/s1387-1811(98)00057-2

Lawton, S.L., Fung, A.S., Kennedy, G.J., Alemany, L.B., Chang, C.D., Hatzikos, G.H., Lissy, D.N., Rubin, M.K., Timken, H.K.C., Steuernagel, S., Woessner, D.E.: Zeolite MCM-49: a three-dimensional MCM-22 analogue synthesized by in situ crystallization. J. Phys. Chem. **100**(9), 3788–3798 (1996). doi:10.1021/jp952871e

Leonowicz, M.E., Lawton, J.A., Lawton, S.L., Rubin, M.K.: MCM-22—a molecular-sieve with 2 independent multidimensional channel systems. Science **264**(5167), 1910–1913 (1994). doi:10.1126/science.264.5167.1910

Meloni, D., Laforge, S., Martin, D., Guisnet, M., Rombi, E., Solinas, V.: Acidic and catalytic properties of H-MCM-22 zeolites 1. Characterization of the acidity by pyridine adsorption. Appl. Catal. A **215**(1–2), 55–66 (2001). doi:10.1016/s0926-860x(01)00501-4

Milanesio, M., Croce, G., Viterbo, D., Pastore, H.O., Mascarenhas, A.J.D., Munsignatti, E., Meda, L.: A combined high-resolution X-ray powder diffraction, computational, and XPS study of the local structure of extra-framework copper ions in over-exchanged Cu-MCM22 zeolite. J. Phys. Chem. A **112**(36), 8403–8410 (2008)

Mortier, W.J.: Compilation of extra-framework sites in zeolites. Butterworths, London (1982)

Nachtigall, P., Bulanek, R.: Theoretical investigation of site-specific characteristics of CO adsorption complexes in the Li^+-FER zeolite. Appl. Catal. A **307**(1), 118–127 (2006)

Nachtigall, P., Delgado, M.R., Nachtigallova, D., Arean, C.O.: The nature of cationic adsorption sites in alkaline zeolites-single, dual and multiple cation sites. Phys. Chem. Chem. Phys. **14**(5), 1552–1569 (2012). doi:10.1039/c2cp23237e

Nachtigall, P., Frolich, K., Drobna, H., Bludsky, O., Nachtigallova, D., Bulanek, R.: FTIR study of CO interactions with Li^+ions in micro- and mesoporous matrices: coordination and localization of Li^+ions. J. Phys. Chem. C **111**(30), 11353–11362 (2007)

Nachtigallova, D., Bludsky, O., Arean, C.O., Bulanek, R., Nachtigall, P.: The vibrational dynamics of carbon monoxide in a confined space-CO in zeolites. Phys. Chem. Chem. Phys. **8**(42), 4849–4852 (2006)

Nachtigallova, D., Nachtigall, P., Bludsky, O.: Calculations of the site specific stretching frequencies of CO adsorbed on Li^+/ZSM-5. Phys. Chem. Chem. Phys. **6**(24), 5580–5587 (2004)

Nicolopoulos, S., Corma, A., Corell, C., Perezpariente, J., Valletregi, M., Gonzalezcalbet, J.M.: Electron microdiffraction and TEM study of the new MCM 22 zeolite. Electron Microscopy 1994, Vols 2a and 2b: Applications in Materials Sciences, pp. 823–824 (1994)

Olson, D.H.: The crystal-structure of dehydrated NaX. Zeolites **15**(5), 439–443 (1995)

Onida, B., Geobaldo, F., Testa, F., Crea, F., Garrone, E.: FTIR investigation of the interaction at 77 K of diatomic molecular probes on MCM-22 zeolite. Microporous Mesoporous Mater. **30**(1), 119–127 (1999)

Palella, B., Pirone, R., Russo, G., Albuquerque, A., Pastore, H.O., Cadoni, M., Frache, A., Marchese, L.: On the activity and hydrothermal stability of CuMCM-22 in the decomposition of nitrogen oxides: a comparison with CuZSM-5. Catal. Commun. **5**, 191–194 (2004)

Pawlesa, J., Zukal, A., Cejka, J.: Synthesis and adsorption investigations of zeolites MCM-22 and MCM-49 modified by alkali metal cations. Adsorpt. J. Int. Adsorpt. Soc. **13**(3–4), 257–265 (2007)

Roth, W.J., Cejka, J.: Two-dimensional zeolites: dream or reality? Catal. Sci. Technol. **1**(1), 43–53 (2011). doi:10.1039/C0CY00027B

Roth, W.J., Kresge, C.T., Vartuli, J.C., Leonowicz, M.E., Fung, A.S., McCullen, S.B.: MCM-36: The first pillared molecular sieve with zeolite properties. Stud. Surf. Sci. Catal. **94**, 301–308 (1995)

Sillar, K., Burk, P.: Adsorption of carbon monoxide on Li-ZSM-5: theoretical study of complexation of Li^+cation with two CO molecules. Phys. Chem. Chem. Phys. **9**(7), 824–827 (2007)

Umamaheswari, V., Hartmann, M., Poppl, A.: EPR spectroscopy of Cu(I)-NO adsorption complexes formed over Cu-ZSM-5 and Cu-MCM-22 zeolites. J. Phys. Chem. B **109**(4), 1537–1546 (2005). doi:10.1021/jp046907r

Wang, S.B., Li, H., Xu, L.Y.: Application of zeolite MCM-22 for basic dye removal from wastewater. J. Colloid Interface Sci. **295**(1), 71–78 (2006). doi:10.1016/j.jcis.2005.08.006

Yang, J., Zhou, Y., Yang, J.Y., Lin, W.G., Wu, Y.J., Lin, N., Wang, J., Zhu, J.H.: Capturing nitrosamines by zeolite MCM-22: effect of zeolite structure and morphology on adsorption. J. Phys. Chem. C **114**(21), 9588–9595 (2010). doi:10.1021/jp9116497

Yang, S.T., Kim, J.Y., Kim, J., Ahn, W.S.: CO_2 capture over amine-functionalized MCM-22, MCM-36 and ITQ-2. Fuel **97**, 435–442 (2012). doi:10.1016/j.fuel.2012.03.034

Zecchina, A., Arean, C.O.: Diatomic molecular probes for mid-IR studies of zeolites. Chem. Soc. Rev. **25**(3), 187–197 (1996)

Zukal, A., Dominguez, I., Mayerova, J., Cejka, J.: Functionalization of delaminated zeolite ITQ-6 for the adsorption of carbon dioxide. Langmuir **25**(17), 10314–10321 (2009a)

Zukal, A., Pawlesa, J., Cejka, J.: Isosteric heats of adsorption of carbon dioxide on zeolite MCM-22 modified by alkali metal cations. Adsorpt. J. Int. Adsorpt. Soc. **15**(3), 264–270 (2009b)